Structural and Magnetic Characterization of Trinuclear, Mixed-Valence Manganese Acetates

Dimitris P. Kessissoglou,[1,2] Martin L. Kirk,[3] Myoung Soo Lah,[2] Xinhua Li,[2] Catherine Raptopoulou,[1] William E. Hatfield,*[,3] and Vincent L. Pecoraro*[,2]

Departments of Chemistry, University of Michigan, Ann Arbor, Michigan 48109, and University of North Carolina, Chapel Hill, North Carolina 27514

Received October 11, 1991

Four mixed valence, trinuclear manganese complexes of general stoichiometry $Mn^{II}Mn^{III}_2L_2(carboxylate)_4X_2$, where L is a tridentate Schiff base ligand and X is a neutral monodentate donor, have been structurally characterized by using X-ray crystallography. The solid-state magnetic behavior of these compounds and two additional isostructural complexes are defined by examining the variable-temperature magnetic susceptibilities of each compound. The structurally characterized complexes have strictly 180° Mn(III)–Mn(II)–Mn(III) angles as required by crystallographic inversion symmetry. These linear complexes, α-$Mn_3(SALADHP)_2(acetate)_4(CH_3OH)_2$ (**1**), α-$Mn_3(SALADHP)_2(acetate)_4(H_2O)_2$ (**2**), α-$Mn_3(SALATHM)_2(acetate)(CH_3OH)_2$ (**3**), and α-$Mn_3(SALADHP)_2(acetate)_4(HpyrO)_2$ (**4**) (where $H_2SALADHP$ = 1,3-dihydroxy-2-methyl-2-(salicylideneamino)propane, $H_2SALATHM$ = tris(hydroxymethyl)(salicylideneamino)methane and HpyrO = 1-aza-2-keto-3,5-cyclohexadiene), are distinguished from the previously reported bent isomer β-$Mn_3(SALADHP)_2(acetate)_4(CH_3OH)_2$ (**5**). The complexes are valence trapped with two terminal Mn(III) ions showing Jahn-Teller distortions along the carboxylate–Mn(III)–X axis. The manganese separations range from 3.42–3.55 Å. This is the first homologous series of mixed-valence complexes that can be used to investigate magnetostructural relationships within manganese clusters. All of the complexes have $S = {}^3/_2$ ground states with $J_{12} \approx -3$ to -7 cm^{-1}, $J_{11'} \approx 0$ cm^{-1}, $z_{j'} \approx 0.3$ cm^{-1}, $g_1 \approx 2.04$, and g_2 fixed at 2.0. Thus, the antiferromagnetic exchange in these complexes is insensitive to changes in metal–metal distance, metal–metal orientation, acetate bridiging groups, phenolate ring substitution, axial ligation, or Mn(III) out of plane displacement. Crystal data for **1**: monoclinic, $P2_1/c$, a = 12.450 (3) Å, b = 13.504 (4) Å, c = 13.428 (5) Å, β = 102.53 (2)°, V = 2203 (1) Å^3. For 3420 data collected between $3 \le 2\theta \le 45°$ and 2111 data $> 3\sigma(I)$, the structure refined to R = 0.057 (R_w = 0.055); Z = 2. Crystal data for **2**: triclinic, $P\bar{1}$, a = 9.459 (10) Å, b = 10.524 (6) Å, c = 10.965 (10) Å, α = 109.55 (6)°, β = 95.65 (8)°, γ = 96.53 (7)°, V = 1011 (2) Å^3, Z = 1. For 2671 data collected between $3 \le 2\theta \le 45°$ and 2010 data $> 3\sigma(I)$, the structure refined to R = 0.041 (R_w = 0.040). Crystal data for **3**: triclinic, $P\bar{1}$, a = 8.694 (3) Å, b = 9.779 (3) Å, c = 14.474 (3) Å, α = 105.53 (2)°, β = 104.30 (2)°, γ = 95.72 (2)°, V = 1130.6 (8) Å^3, Z = 1. For 3174 data collected between $3 \le 2\theta \le 45°$ and 2321 data $> 3\sigma(I)$ the structure refined to R = 0.041 (R_w = 0.040). Crystal data for **4**: triclinic, $P\bar{1}$, a = 10.025 (4) Å, b = 13.302 (8) Å, c = 13.380 (7) Å, α = 114.48 (4)°, β = 96.57 (4)°, γ = 112.33 (4)°, V = 1422 (1) Å^3, Z = 1. For 3727 data collected between $3 \le 2\theta \le 40°$ and 2502 data $> 3\sigma(I)$, the structure refined to R = 0.057 (R_w = 0.063).

Introduction

Efforts to model the active site of the OEC have resulted in many interesting new structural types for mixed-valence clusters of manganese.[4-17] We have described the coordination chemistry of mononuclear Mn(IV)[18] and dinuclear[19] complexes using dominantly or entirely oxygen-derived donors. Many of the structurally characterized model compounds have been tetranuclear[9,11,13-15] while a few trinuclear materials have appeared.[5-7,20] In this contribution we describe the structures of six mixed-valence trinuclear complexes that primarily use an oxygen donor set to the metal. These materials are of general formula $Mn^{III}_2Mn^{II}L_2(OAc)_4X_2$ and represent an interesting structural class for

(1) Present Address: Department of General and Inorganic Chemistry, Aristotelian University of Thessaloniki, Thessaloniki, Greece 54006.
(2) University of Michigan.
(3) University of North Carolina.
(4) Recent reviews of this subject include the following: (a) Babcock, G. T.; Barry, B. A.; Debus, R. J.; Hoganson, C. W.; Atamain, M.; McIntosh, L.; Sithole, I.; Yocum, C. F. *Biochemistry* **1989**, *28*, 9557. (b) Rutherford, A. W. *Trends Biochem. Sci.* **1989**, *14*, 227. (c) Ghanotakis, D. F.; Yocum, C. F. *Annu. Rev. Plant Physiol.*, in press. (d) Christou, G. *Acc. Chem. Res.* **1989**, *22*, 328. (e) Pecoraro, V. L. *Photochem. Photobiol.* **1988**, *48*, 249. (f) Wieghardt, K. *Angew. Chem., Int. Ed. Engl.* **1990**, *28*, 1153. (g) Govindjee; Coleman, W. J. *Sci. Am.* **1990**, *262*, 50.
(5) Li, X.; Kessissoglou, D. P.; Kirk, M. L.; Bender, C. A.; Pecoraro, V. L. *Inorg. Chem.* **1988**, *27*, 1.
(6) Kessissoglou, D. P.; Lah, M. S.; Kirk, M. L.; Bender, C. A.; Pecoraro, V. L. *J. Chem. Soc., Chem. Commun.* **1989**, 84.
(7) Vincent, J. B.; Chang, H. R.; Folting, K.; Huffman, J. C.; Christou, G.; Hendrickson, D. N. *J. Am. Chem. Soc.* **1987**, *109*, 5703.
(8) Wieghardt, K.; Bossek, U.; Zsolnai, L.; Huttner, G.; Blondin, G.; Girerd, J.-J.; Babonneau, F. *J. Chem. Soc., Chem. Commun.* **1987**, 651.
(9) Vincent, J. B.; Christmas, C.; Huffman, J. C.; Christou, G.; Chang, H.-R.; Hendrickson, D. N. *J. Chem. Soc., Chem. Commun.* **1987**, 236.
(10) Wieghardt, K.; Bossek, V.; Ventur, D.; Weiss, J. *J. Chem. Soc., Chem. Commun.* **1985**, 347.
(11) Bashkin, J. S.; Chang, H. R.; Streib, W. E.; Huffman, J. C.; Hendrickson, D. N.; Christou, G. *J. Am. Chem. Soc.* **1987**, *109*, 6502.
(12) Sheats, J. E.; Czernuszewicz, R. S.; Dismukes, G. C.; Rheingold, R. H.; Petrouleas, V.; Stubbe, J.; Armstrong, W. M.; Lippard, S. J. *J. Am. Chem. Soc.* **1987**, *109*, 1435.
(13) Wieghardt, K.; Bossek, V.; Gebert, W. *Angew. Chem., Int. Ed. Engl.* **1983**, *22*, 328.
(14) Kulawiec, R. J.; Crabtree, R. H.; Brudvig, G. W.; Schulte, G. K. *Inorg. Chem.* **1988**, *27*, 1309.
(15) McKee, V.; Shepard, W. B. *J. Chem. Soc., Chem. Commun.* **1985**, 158. (b) Brooker, S.; McKee, V.; Shepard, W. B.; Pannell, L. *J. Chem. Soc., Dalton Trans.* **1987**, 2555.
(16) Basu, P.; Pal, S.; Chakravorty, A. *Inorg. Chem.* **1988**, *27*, 1850.
(17) Seela, J. L.; Folting, K.; Wang, J.-R.; Huffman, J. C.; Christou, G.; Chang, H.-R.; Hendrickson, D. N. *Inorg. Chem.* **1985**, *24*, 4454.
(18) (a) Kessissoglou, D. P.; Butler, W. M.; Pecoraro, V. L. *J. Chem. Soc., Chem. Commun.* **1986**, 1253. (b) Kessissoglou, D. P.; Li, X.; Butler, W. M.; Pecoraro, V. L. *Inorg. Chem.* **1987**, *26*, 2487. (c) Li, X.; Lah, M. S.; Pecoraro, V. L. *Acta Crystallogr.* **1989**, *C45*, 1517. (d) Saadeh, S. M.; Lah, M. S.; Pecoraro, V. L. *Inorg. Chem.* **1991**, *30*, 9.
(19) (a) Bonadies, J. A.; Lah, M. S.; Kirk, M. L.; Kessissoglou, D. P.; Hatfield, W.; Pecoraro, V. L. *Inorg. Chem.* **1989**, *28*, 2037. (b) Bonadies, J. A.; Maroney, M. L.; Pecoraro, V. L. *Inorg. Chem.* **1989**, *28*, 2044. (c) Larson, E.; Pecoraro, V. L. *J. Am. Chem. Soc.* **1991**, *113*, 3810. (d) Larson, E.; Lah, M. S.; Li, X.; Bonadies, J. A.; Pecoraro, V. L. *Inorg. Chem.* **1992**, *31*, 373. (e) Larson, E. L.; Riggs, P.; Penner-Hahn, J. E.; Pecoraro, V. L. *J. Chem. Soc., Chem. Commun.* **1992**, 102. (f) Larson, E. L.; Haddy, A.; Kirk, M. L.; Sands, R.; Hatfield, W.; Pecoraro, V. L. *J. Am. Chem. Soc.* **1992**, *114*, 6263.

0020-1669/92/1331-5424$03.00/0

manganese Schiff base compounds. We have evaluated the effects of axial ligation, metal separation and angular orientation, altered bridging ligands, and phenolate ring substitution on the spin exchange in these trinuclear molecules by examining the temperature dependence of the magnetic susceptibilities. From this study we conclude that for this class of mixed-valence cluster, the weak magnetic coupling and $S = {}^3/_2$ ground electronic states are insensitive to all of these perturbations. Apparently, major structural rearrangements are required to significantly modify the exchange interaction in these linear and bent complexes. In a separate report,[21] we will provide the solution characterization of these trinuclear species in a variety of solvents (including EPR and ^{1}H NMR spectroscopies and electrochemistry) and demonstrate how, depending on the extent of dissociation in different solvents, trinuclear-derived complexes can give rise to both low-field ($g \geq 4$) and $g = 2$ multiline type EPR spectral features.

Experimental Section

The following abbreviations are used throughout the text: H_2-SALADHP = 1,3-dihydroxy-2-methyl-2-(salicylideneamino)propane; 5-Cl-H_2SALADHP = 1,3-dihydroxy-2-methyl-2-(5-chlorosalicylideneamino)propane; H_2SALAHP = 1-hydroxy-3-(salicylideneamino)propane; H_2SALATHM = tris(hydroxymethyl)(salicylideneamino)methane; H_2-SAL = salicylic acid; HOAc = acetic acid; PyrOH = 2-hydroxypyridine; HpyrO = 1-aza-2-keto-3,5-cyclohexadiene; H_2HIB = 2-hydroxyisobutyric acid; 2-OH-SALPN = 2-hydroxybis(salicylidene)propylenediamine; SALGLY = salicylideneglycine.

Materials. Salicylaldehyde, salicylic acid, and 2-hydroxypyridine were purchased from Aldrich Chemical Co. 2-Amino-2-methyl-1,3-propanediol, $Mn(OAc)_3 \cdot 2H_2O$, and $Mn(OAc)_2 \cdot 4H_2O$ were obtained from Fluka Chemical Co. Tris(hydroxymethyl)aminomethane was obtained from Sigma Chemical Co. All other chemicals and solvents were reagent grade. Elemental analyses were performed by Galbraith Analytical Laboratories, Inc., Knoxville, TN.

Synthesis of Compounds. α-[$Mn^{II}Mn^{III}_2$(SALADHP)$_2$(OAc)$_4$(CH_3OH)$_2$]·2CH_2OH (1). Twenty millimoles of salicylaldehyde (2.16 mL) was added to a methanol solution of 20 mmol of 2-amino-2-methyl-1,3-propanediol (2.10 g) and refluxed for 1 h, resulting in a pale yellow solution. After the solution was cooled to room temperature, 30 mmol of $Mn(OAc)_2 \cdot 4H_2O$ (7.35 g) was added with stirring. This reaction mixture was refluxed for 4 h, after which the solution was allowed to cool to room temperature and was exposed to dioxygen by bubbling air into the reaction mixture. Dichroic (green/red) crystals suitable for X-ray diffraction studies were obtained by slow evaporation. A deep red powder was collected if the reaction mixture was initially reduced to one-third its original volume. IR, elemental analysis, ^{1}H NMR, and all other physical studies carried out on the red powder showed it to be identical to the dichroic crystals. The yield of **1** based on manganese is 80%. Anal. Calcd for $Mn_3C_{34}H_{54}N_2O_{18}$ (MW = 943): C, 43.27; H, 5.73; N, 2.97; Mn, 17.5. Found: C, 43.66; H, 5.37; N, 3.01; Mn, 17.20.

α-[$Mn^{II}Mn^{III}_2$(SALADHP)$_2$(OAc)$_4$(H_2O)$_2$]·2H_2O·2CH_3OH (2). Twenty millimoles of **1** was dissolved in 75 mL of methanol. To this solution was added 20 mL of water and the reaction mixture stirred overnight. Slow evaporation afforded X-ray quality crystals of **2**. A comparison of the IR spectra of **1** and **2** showed that the complexes were similar, but not identical. The yield of **2** based on manganese is 60%. Anal. Calcd for $Mn_3C_{32}H_{54}N_2O_{20}$ (MW = 951.6): C, 40.35; H, 5.67; N, 2.94; Mn, 17.34; Found: C, 40.14; H, 5.39; N, 2.81; Mn, 17.89.

α-[$Mn^{II}Mn^{III}_2$(SALATHM)$_2$(OAc)$_4$(CH_3OH)$_2$]·H_2O·2CH_3OH (3). This compound was synthesized by a procedure analogous to that of **1** except that tris(hydroxymethyl)aminomethane was substituted for 2-amino-2-methyl-1,3-propanediol. X-ray quality crystals were obtained by slow evaporation of a methanol solution. The yield of **3** based on manganese is 80%. Anal. Calcd for $Mn_3C_{34}H_{58}N_2O_{22}$ (MW = 1011): C, 40.36; H, 5.74; N, 2.77; Mn, 16.32. Found: C, 39.81; H, 5.27; N, 2.75; Mn, 16.73.

α-[$Mn^{II}Mn^{III}_2$(SALADHP)$_2$(OAc)$_4$(HpyrO)$_2$]·H_2O·2HOpyr (4). Twenty millimoles of **1** was dissolved in 75 mL of methanol. To this solution was added an excess of 2-hydroxypyridine and the reaction mixture stirred overnight. Slow evaporation afforded X-ray quality crystals of **5**. The yield of **5** based on manganese is 40%. Anal. Calcd for $Mn_3C_{50}H_{62}N_6O_{19}$ (MW = 12.11.9): C, 49.46; H, 4.95; N, 6.92; Mn, 13.60. Found: C, 48.70; H, 5.00; N, 6.79; Mn, 14.02.

β-[$Mn^{II}Mn^{III}_2$(SALADHP)$_2$(OAc)$_4$(CH_3OH)$_2$]·4HOpyr (5). Twenty millimoles of **1** was dissolved in 5 mL of methanol. To this solution was added 75 mL of acetonitrile and 40 mmol of 2-hydroxypyridine. The reaction mixture was then stirred overnight. Slow evaporation afforded X-ray quality crystals of **5** with a yield based on manganese of 80%. A previous report of this structure has appeared.[6] Anal. Calcd for $Mn_3C_{52}H_{66}N_6O_{20}$ (MW = 1255.4): C, 49.56; H, 5.24; N, 6.67; Mn, 13.10. Found: C, 49.80; H, 5.32; N, 6.46; Mn, 13.89.

α-[$Mn^{II}Mn^{III}_2$(SALADHP)$_2$(OAc)$_2$(Hsal)$_2$(CH_3CH_2OH)$_2$]·4H_2O (6). Twenty millimoles of **1** was dissolved in 75 mL of ethanol. To this solution was added 80 mmol of salicylic acid and of $KMnO_4$. Slow evaporation afforded black crystals that were subsequently shown to contain infinite chains of $[K_2Mn_2(sal)_4(CH_3OH)_2]_n$ that was reported[22] separately. After filtration of these crystals, a new crystal type, **6**, was observed that had an IR spectrum more similar to those of the previously isolated trinuclear complexes.[5,6] The yield of **6** based on manganese is 40%. Anal. Calcd for $Mn_3C_{44}H_{62}N_2O_{20}$ (MW = 1103): C, 47.87; H, 5.62; N, 2.54; Mn, 14.96. Found: C, 47.79; H, 5.48; N, 2.48; Mn, 14.6.

Collection and Reduction of X-ray Data. Suitable crystals of the compounds **1**–**4** and **6** were obtained as described above and mounted in glass capillaries. Intensity data were obtained at room temperature on a Syntex $P2_1$ diffractometer using Mo Kα radiation (0.7107 Å) monochromatized from a graphite crystal whose diffraction vector was parallel to the diffraction vector of the sample. Three standard reflections were measured every 50 reflections. The crystal and data parameters are given in Table I. Intensity data were collected using $\theta/2\theta$ scans. Crystal faces were measured, and a numerical absorption correction was applied to each data set. The data were reduced using the SHELEX76 program package[23] and the structures solved using SHELEX86. The SHELEX76 program was used for subsequent refinement of the model for each structure. Atomic scattering factors used were from ref 23b. Hydrogen atoms were located, but not refined, and placed at fixed distances of 0.95 Å from bonded carbon atoms in the final difference map of each complex. Unique data and final R indices are reported in Table I. Fractional atomic coordinates are reported as Tables II–V, a selected list of chemically equivalent bond lengths and angles are given in Table VI, and specific distances and angles for five complexes are provided in Table VII.

Spectroscopic and Magnetic Measurements. Infrared spectra were recorded on a Nicolet 60SX Fourier transform spectrometer with samples prepared as KBr pellets. Magnetic susceptibility data were collected by using a Princeton Applied Research Model 155 Foner vibrating sample magnetometer using procedures that have been described earlier.[24] The magnetometer was calibrated with $HgCo(NCS)_4$.[25,26] Samples of the standard and the compounds under study were contained in precision milled Lucite sample holders. Approximately 150 mg of each were used. Isothermal magnetization measurements were made by using the PAR vibrating sample magnetometer with the temperature in the sample chamber being controlled by a Keithley 227 constant current source control. Temperatures were measured as described for the magnetic susceptibility measurements, and constant magnetic fields were controlled by using the FFC-4 field control unit with the Magnion precision magnet power supply. Magnetic susceptibility measurements in the temperature range 77–300 K were made with a Faraday balance operated as an alternating force magnetometer. The system consisted of a Cahn 2000

(20) (a) Shibata, S.; Onuma, S.; Inoue, H. *Inorg. Chem.* **1985**, *24*, 1723. Murray, B. D.; Hope, H.; Power, P. P. *J. Am. Chem. Soc.* **1985**, *107*, 169. Bhula, R.; Gainsford, G. J.; Weatherburn, D. C. *J. Am. Chem. Soc.* **1988**, *110*, 7550. (b) Auger, N.; Girerd, J.-J.; Corbella, M.; Gleizes, A.; Zimmerman, J.-L. *J. Am. Chem. Soc.* **1990**, *112*, 448.
(21) Li, X.; Bonadies, J. A.; Kessissoglou, D. P.; Bender, C.; Pecoraro, V. L. Manuscript in preparation.
(22) Kirk, M. L.; Lah, M. S.; Raptopoulou, C.; Kessissoglou, D. P.; Hatfield, W. E.; Pecoraro, V. L. *Inorg. Chem.* **1991**, *30*, 3900.
(23) (a) Computations were carried out on an Amdahl 5860 computer. Computer programs used during structural analysis were from the SHELEX program package by George Sheldrick, Institute fur Anorganische Chemie der Universitat Gottingen, Federal Republic of Germany. Other programs used include ORTEP, a thermal ellipsoidal drawing program by C. K. Johnson, and the direct methods program MULTAN78 by Peter Main. (b) *International Tables for X-ray Crystallography*; Ibers, J., Hamilton, W., Eds.; Kynoch: Birmingham, England, 1974; Vol. IV, Tables 2.2 and 2.3.1.
(24) Corvan, P. J.; Estes, W. E.; Weller, R. R.; Hatfield, W. E. *Inorg. Chem.* **1980**, *19*, 1297.
(25) Figgis, B. N.; Nyholm, R. S. *J. Chem. Soc.* **1958**, 4190.
(26) Brown, D. B.; Crawford, V. H.; Hall, J. W.; Hatfield, W. E. *J. Phys. Chem.* **1977**, *81*, 1303.

Table I. Summary of Crystallographic Data for Compounds **1–4**

	1	2	3	4
formula	$Mn_3C_{34}H_{54}N_2O_{18}$	$Mn_3C_{32}H_{54}N_2O_{20}$	$Mn_3C_{34}H_{58}N_2O_{22}$	$Mn_3C_{50}H_{62}N_6O_{19}$
MW	939.6	951.6	1011	1211.9
space group	$P2_1/c$ (No. 14)	$P\bar{1}$ (No. 2)	$P\bar{1}$ (No. 2)	$P\bar{1}$ (No. 2)
a, Å	12.450 (3)	9.459 (10)	8.694 (3)	10.025 (4)
b, Å	13.502 (4)	10.524 (6)	9.779 (3)	13.302 (8)
c, Å	13.428 (5)	10.965 (10)	14.474 (3)	13.380 (7)
α, deg		109.55 (6)	105.53 (2)	114.48 (4)
β, deg	102.53 (2)	95.65 (8)	104.30 (2)	96.57 (4)
γ, deg		96.53 (7)	95.72 (2)	112.33 (4)
V, Å^3	2220.3 (1)	1011 (2)	1130.6 (4)	1422 (1)
Z	2	1	1	1
T, (°C)	23	23	23	23
λ, Å	0.7104	0.7104	0.7104	0.7104
ρ_{calcd}, g/cm^3	1.422	1.563	1.468	1.415
ρ_{obsd}, g/cm^3	1.42 (1)	1.52 (1)	1.47 (1)	1.39 (1)
μ, cm^{-1}	8.84	9.32	8.38	6.72
R^a	0.057	0.041	0.041	0.058
$R_w{}^b$	0.055	0.040	0.040	0.064

$^a R = \sum||F_o| - |F_c||/|F_o|$. $^b R_w = [\sum w(|F_o| - |F_c|)^2/\sum w|F_o|^2]^{1/2}$.

Table II. Fractional Atomic Coordinates for **1**

atom	x	y	z	U, Å^2
Mn1	1.0000 (0)	0.5000 (0)	1.0000 (0)	0.041
Mn2	0.9823 (2)	0.3771 (2)	0.7666 (2)	0.042
O1	0.9289 (7)	0.2832 (7)	0.6649 (7)	0.051
C1	0.9791 (10)	0.2333 (10)	0.6042 (10)	0.042
C2	0.9173 (12)	0.1729 (14)	0.5288 (12)	0.067
C3	0.9645 (15)	0.1211 (16)	0.4623 (14)	0.095
C4	1.0780 (15)	0.1243 (17)	0.4706 (15)	0.109
C5	1.1412 (13)	0.1828 (13)	0.5432 (13)	0.073
C6	1.0937 (11)	0.2392 (10)	0.6105 (10)	0.043
C7	1.1653 (10)	0.2994 (10)	0.6823 (10)	0.041
N1	1.1353 (8)	0.3606 (8)	0.7449 (8)	0.044
C8	1.2185 (11)	0.4221 (12)	0.8148 (11)	0.056
C9	1.1493 (12)	0.5114 (11)	0.8368 (11)	0.055
O2	1.0485 (7)	0.4765 (6)	0.8581 (6)	0.043
C10	1.2613 (11)	0.3618 (13)	0.9123 (12)	0.064
C11	1.3179 (23)	0.4524 (21)	0.7727 (18)	0.092
O3	0.8286 (7)	0.4014 (7)	0.7731 (7)	0.052
O4	0.8273 (7)	0.4812 (8)	0.9183 (8)	0.054
C12	0.7818 (11)	0.4449 (11)	0.8360 (12)	0.043
C13	0.6576 (11)	0.4489 (12)	0.8049 (11)	0.056
O5	0.9989 (7)	0.2669 (7)	0.8850 (7)	0.051
O6	1.0183 (8)	0.3432 (7)	1.0370 (7)	0.055
C14	1.0226 (11)	0.2677 (11)	0.9822 (12)	0.046
C15	1.0626 (14)	0.1731 (12)	1.0357 (13)	0.068
O7	0.9517 (9)	0.5058 (8)	0.6464 (8)	0.068
O8	1.3235 (10)	0.4166 (13)	0.9914 (11)	0.069
O8′	0.2939 (64)	0.4955 (49)	−0.2911 (66)	0.182
C16	0.8738 (15)	0.5040 (16)	0.5497 (14)	0.089
O9	0.9238 (20)	0.6694 (16)	0.7555 (14)	0.091
C17	0.7813 (37)	0.7133 (34)	0.7300 (32)	0.165
O9′	−0.1436 (49)	0.6534 (36)	−0.2511 (35)	0.090
C17′	0.0084 (82)	0.7241 (76)	−0.2435 (68)	0.153

Table III. Fractional Atomic Coordinates for **2**

atom	x	y	z	U, Å^2
Mn1	0.0 (0)	0.0 (0)	0.0 (0)	0.018
Mn2	0.0864 (1)	−0.2355 (1)	0.1352 (1)	0.032
O1	0.0492 (4)	−0.3609 (4)	0.2209 (4)	0.040
O2	0.1443 (4)	−0.1074 (4)	0.0574 (4)	0.032
O3	−0.0970 (4)	−0.3247 (4)	0.0201 (4)	0.037
O4	−0.1555 (5)	−0.1699 (4)	−0.0658 (4)	0.044
O5	−0.0337 (4)	−0.0979 (4)	0.2648 (4)	0.043
O6	−0.0721 (5)	0.0640 (4)	0.1828 (4)	0.046
O7	0.1898 (6)	−0.3926 (5)	−0.0107 (5)	0.047
O8	0.3609 (6)	0.1022 (5)	0.4439 (5)	0.061
N1	0.2787 (5)	−0.1601 (5)	0.2454 (5)	0.032
C1	0.1349 (7)	−0.3915 (6)	0.3056 (6)	0.037
C2	0.0862 (7)	−0.5051 (7)	0.3389 (7)	0.050
C3	0.1701 (8)	−0.5411 (7)	0.4272 (7)	0.061
C4	0.3066 (8)	−0.4675 (7)	0.4847 (7)	0.057
C5	0.3562 (7)	−0.3580 (6)	0.4538 (6)	0.043
C6	0.2727 (6)	−0.3172 (6)	0.3638 (5)	0.032
C7	0.3370 (6)	−0.2033 (6)	0.3335 (6)	0.036
C8	0.3565 (6)	−0.0417 (6)	0.2208 (6)	0.036
C9	0.2961 (6)	−0.0659 (6)	0.0789 (6)	0.037
C10	0.3142 (7)	0.0896 (6)	0.3121 (6)	0.038
C11	0.5186 (8)	−0.0359 (9)	0.2350 (8)	0.057
C12	−0.0686 (6)	0.0145 (6)	0.2728 (6)	0.033
C13	−0.1096 (9)	0.0989 (8)	0.4009 (7)	0.047
C14	−0.1821 (7)	−0.2784 (6)	−0.0466 (6)	0.035
C15	−0.3260 (8)	−0.3641 (9)	−0.1032 (9)	0.055
O9	0.2355 (6)	−0.2818 (5)	−0.2091 (5)	0.069
O10	0.2189 (8)	0.2459 (7)	0.6278 (6)	0.090
C17	0.3003 (11)	0.3538 (10)	0.7300 (10)	0.078

microbalance, an ANAC series 3472 100 mm electromagnet with planar pole pieces, and George Associates Model 502 Lewis coils to provide the field gradient. The Lewis coils were powered by a George Associates Model 202 bipolar current regulated power source, and the electromagnet was powered and regulated by an ANAC Model 3610-I control system and a Sorensen SRL 40-50 power supply. The system was interfaced to a Tektronix 4052 microcomputer through a Hewlett-Packard 3495A scanner and a Fluke 8502A digital multimeter. Samples were contained in polycarbonated capsules obtained from Universal Plastics and Engineering Co., and they were suspended from the electrobalance by a fine gold chain. The Faraday system was calibrated by using $HgCo(NCS)_4$.[25,26] Temperatures were measured by using a Lake Shore Cryotronics DT-500 silicon diode. A correction for the diamagnetism of the constituent atoms were estimated from Pascal's constants.[27-29]

The fitting calculations were carried out by using a Simplex nonlinear least-squares fitting program,[30] with the criterion of best fit being the minimum value of the function

$$F = \sum_i \frac{[\chi_i{}^{obsd}T_i - \chi_i{}^{calcd}T_i]^2}{[\chi_i{}^{obsd}T_i]^2}$$

Results

Synthesis of Compounds. Trinuclear, mixed-valence complexes of the general composition $Mn^{II}Mn^{III}{}_2L_2(carboxylate)_4X_2$ can be isolated by a variety of synthetic methods using a wide range of tridentate Schiff base ligands (L), carboxylate donors and neutral axial ligands (X). The linear adducts, designated α isomers and defined by the rigorous Mn(III)–Mn(II)–Mn(III) angle of 180° (vide infra), are best prepared by the reaction of 1.5 equiv of manganese(II) acetate with 1.0 equiv of tridentate Schiff base ligand, such as SALADHP, in methanol using air as an oxidant. From this reaction mixture, compound **1** can be

(27) Ro, H.-K.; Kirk, M. L.; Hatfield, W. E. To be published.
(28) Figgis, B. N.; Lewis, J. In *Modern Coordination Chemistry*; Lewis, J., Wilkins, R. L., Eds.; New York: Interscience; 1960; Chapter 6.
(29) Weller, R. R.; Hatfield, W. E. *J. Chem. Educ.* **1979**, *56*, 652.
(30) (a) Spendley, W.; Hexst, G. R.; Himsworth, F. R. *Technometrics* **1962**, *4*, 441. (b) Nedler, J. A.; Mead, R. *Comput. J.* **1965**, *7*, 308.

Table IV. Fractional Atomic Coordinates for **3**

atom	*x*	*y*	*z*	*U*, Å²
Mn1	0.0 (0)	0.0 (0)	0.0 (0)	0.030
Mn2	0.0916 (1)	0.2052 (1)	0.2527 (1)	0.032
O1	0.1215 (4)	0.3756 (4)	0.3571 (2)	0.042
O2	0.0793 (4)	0.0287 (3)	0.1577 (2)	0.029
O3	0.3155 (5)	−0.1173 (4)	0.3999 (3)	0.053
O4	0.4515 (4)	−0.0601 (4)	0.1394 (3)	0.048
O5	−0.1147 (4)	0.2513 (4)	0.1835 (3)	0.045
O6	−0.1985 (4)	0.1151 (4)	0.0246 (2)	0.043
O7	0.2048 (5)	0.3326 (4)	0.1766 (3)	0.047
O8	0.1493 (4)	0.2026 (4)	0.0168 (3)	0.046
O9	−0.0833 (5)	0.0849 (5)	0.3112 (3)	0.060
O10	0.8808 (7)	0.3711 (5)	0.7147 (4)	0.088
O11	0.2562 (4)	0.1458 (4)	0.8394 (3)	0.054
N1	0.2822 (5)	0.1452 (4)	0.3321 (3)	0.029
C1	0.2173 (6)	0.4191 (6)	0.4509 (4)	0.033
C2	0.1993 (6)	0.5450 (5)	0.5169 (4)	0.035
C3	0.2935 (7)	0.5945 (6)	0.6146 (4)	0.040
C4	0.4158 (7)	0.5230 (6)	0.6487 (4)	0.043
C5	0.4366 (6)	0.3977 (6)	0.5851 (4)	0.040
C6	0.3370 (6)	0.3427 (5)	0.4853 (3)	0.029
C7	0.3644 (6)	0.2112 (5)	0.4241 (4)	0.031
C8	0.3211 (6)	0.0101 (5)	0.2732 (3)	0.030
C9	0.1575 (6)	−0.0712 (5)	0.2014 (3)	0.030
C10	0.4024 (7)	−0.0809 (6)	0.3365 (4)	0.042
C11	0.4325 (6)	0.0568 (6)	0.2169 (4)	0.040
C12	−0.2151 (6)	0.2068 (6)	0.0981 (4)	0.035
C13	−0.3649 (6)	0.2724 (6)	0.0857 (4)	0.047
C14	0.1991 (6)	0.3184 (6)	0.0879 (4)	0.039
C15	0.2577 (8)	0.4509 (6)	0.0625 (5)	0.064
C16	−0.0666 (9)	0.0669 (8)	0.4047 (5)	0.075
C17	0.0567 (11)	0.3757 (9)	0.7297 (7)	0.108

isolated in greater than 80% yield. To obtain this high yield, it is absolutely essential not to add additional strong base such as sodium methoxide or sodium hydroxide. If one does add base, mononuclear Mn(IV) complexes[18] and MnO_2 are formed exclusively. One can also synthesize **1** using appropriate ratios of $MnCl_2$ and sodium acetate. The reaction is less efficient if manganese(III) acetate is the starting material; however, one still can obtain **1** with this salt. We believe that Mn(II) is generated via disproportionation of the Mn(III) in this reaction process.

The initial formation of the trinuclear complex is probably the result of ion pair interactions as the molecule crystallizes. The central manganese(II) is encapsulated by the acetate and alkoxide moieties of $Mn(SALADHP)(OAc)_2^-$, resulting in a neutral complex. We have completely encapsulated sodium in similar environments with either two bridging acetates and four bridging phenolates[19a] as in $\{Na[Mn^{III}(2\text{-OH-SALPN})(OAc)_2]_2\}^-$ or using three alkoxides[18d] as in $\{Na[Mn^{II}(HIB)_3]_2\}^{3-}$. Thus, the weak association of mono and divalent ions to coordinated oxygen atoms that have been described previously by Sinn[31] and Floriani[32] can be exploited to realize new mixed-valence manganese clusters. Once generated, one can stabilize the trinuclear formulation in solution by an appropriate choice of solvent.

A variety of neutral, axial ligands can be accomodated by the Mn(III) ions. The THF and DMF adducts can be prepared directly by using the appropriate solvent rather than methanol. Water can be substituted for methanol by completing the reaction in a 1:3 ratio of water to methanol (Figure 1). Similarly, the addition of an excess of 2-hydroxypyridine to a methanolic solution yields the oxygen bound α-$Mn^{II}Mn^{III}_2(SALADHP)_2(OAc)_4(HpyrO)_2$ (**4**) (Figure 2, vide infra). Substitution of the acetate moieties, for example by $D_3CCO_2^-$, is easily achieved using the $MnCl_2$ reaction with sodium deuterioacetate. Generation of the mixed acetate/salicylate complex is less straightforward. Compound **6** was isolated through fractional crystallization of an

(31) Sinn, E.; Harris, L. M. *Coord. Chem. Rev.* **1969**, *4*, 391.
(32) Arena, F.; Floriani, C.; Zanazzi, P. F. *J. Chem. Soc., Chem. Commun.* **1987**, 183.

Table V. Fractional Atomic Coordinates for **4**

atom	*x*	*y*	*z*	*U*, Å²
Mn1	0.5000 (0)	0.9416 (5)	0.7500 (0)	0.032
Mn2	0.4781 (1)	0.8194 (3)	0.6143 (1)	0.033
O1	0.4821 (6)	0.8344 (13)	0.5435 (5)	0.038
O2	0.4693 (5)	0.7921 (22)	0.6822 (5)	0.029
O3	0.5657 (6)	0.8565 (13)	0.6570 (6)	0.044
O4	0.5839 (6)	0.9445 (13)	0.7432 (6)	0.044
O5	0.4514 (6)	1.0245 (14)	0.6049 (6)	0.048
O6	0.4616 (6)	1.1018 (13)	0.6889 (6)	0.046
O7	0.5079 (6)	0.6003 (14)	0.6175 (6)	0.054
O8	0.2825 (7)	0.8697 (15)	0.5607 (6)	0.072
O9	0.0267 (8)	0.0639 (17)	0.2026 (7)	0.079
O10	0.2537 (8)	1.3862 (19)	0.4610 (7)	0.105
N1	0.3936 (6)	0.7531 (15)	0.5729 (6)	0.029
N2	0.0951 (8)	0.2128 (19)	0.2650 (8)	0.059
N3	0.2990 (8)	1.1882 (20)	0.4696 (7)	0.055
C1	0.4393 (8)	0.8173 (20)	0.4889 (8)	0.032
C2	0.4546 (8)	0.8429 (20)	0.4432 (8)	0.038
C3	0.4127 (10)	0.8213 (23)	0.3848 (9)	0.050
C4	0.3553 (10)	0.7751 (22)	0.3704 (9)	0.056
C5	0.3393 (9)	0.7506 (21)	0.4138 (9)	0.048
C6	0.3810 (8)	0.7695 (18)	0.4742 (8)	0.031
C7	0.3608 (8)	0.7399 (19)	0.5172 (8)	0.035
C8	0.3674 (8)	0.7212 (18)	0.6133 (7)	0.030
C9	0.4237 (8)	0.6997 (20)	0.6731 (7)	0.032
C10	0.3337 (9)	0.8412 (20)	0.6172 (8)	0.037
C11	0.3259 (9)	0.5992 (21)	0.5930 (8)	0.045
C12	0.5993 (9)	0.8996 (20)	0.7077 (9)	0.039
C13	0.6663 (10)	0.9059 (24)	0.7249 (9)	0.061
C14	0.4460 (9)	1.1133 (21)	0.6346 (9)	0.036
C15	0.4201 (9)	1.2430 (22)	0.6058 (9)	0.050
C16	0.4978 (10)	0.5233 (23)	0.5677 (10)	0.066
C17	0.0817 (12)	0.0971 (25)	0.2340 (10)	0.061
C18	0.1299 (11)	0.0162 (23)	0.2372 (10)	0.061
C19	0.1881 (11)	0.0600 (27)	0.2723 (10)	0.073
C20	0.1990 (11)	0.1805 (28)	0.3033 (10)	0.075
C21	0.1530 (12)	0.2565 (25)	0.2996 (10)	0.071
C22	0.3719 (10)	1.1615 (25)	0.4352 (10)	0.067
C23	0.3404 (11)	1.1130 (24)	0.4602 (10)	0.071
C24	0.3249 (11)	1.3705 (26)	0.4265 (10)	0.080
C25	0.3643 (11)	1.2894 (26)	0.4186 (10)	0.071
C26	0.2920 (10)	1.3147 (25)	0.4531 (9)	0.054

ethanol solution containing **1**, salicylic acid, and $KMnO_4$. The first material to crystallize (ρ = 1.55 g/mL), which was reported separately,[22] contained infinite chains of $[K_2Mn_2(sal)_4(CH_3OH)_2]_n$. After filtration, a different crystalline form (ρ = 1.45 g/mL; subsequently shown to be **6**) deposited. Preliminary X-ray characterization of this material confirmed that it was a trinuclear cluster with both acetate and salicylate moieties bridging the Mn(III) and Mn(II) ions. The basic structural motif of **6** has been confirmed; however, because of the poor quality of data, we have refrained from a detailed crsytallographic description.[33]

A structural isomer of **1** with a significant deviation from linearity (Mn(III)–Mn(II)–Mn(III) angle of 138.5 (2)) has previously been isolated from acetonitrile/methanol (7:1) in the presence of 2-hydroxypyridine and structurally characterized (Figure 3).[6] This complex, **5**, which we classified as the β-isomer, was isolated as the sole product of the reaction. The β-isomer was only obtained if both 2-hydroxypyridine and acetonitrile are used. The linear isomer, **1**, was recovered from acetonitrile in the absence of 2-hydroxypyridine, and **4** was obtained if 2-hydroxypyridine was added to a methanol solution.

(33) Crystallographic parameters for **6**: monoclinic, $P2_1/a$, a = 21.926 (6) Å, b = 13.295 (5) Å, c = 18.237 (5) Å, β = 114.19 (2)°, V = 4850 (3) Å³, Z = 4. For 4557 data collected between $3 \le 2\theta \le 40°$ and 2759 data $> 3\sigma(I)$ the structure refined to R = 0.092 (R_w = 0.092). The high R indices for this structure are a result of the disorder in the salicylate molecules and the lack of sufficient data to refine all atoms anisotropically (only the manganese and heteroatoms were refined anisotropically, all other atoms were refined isotropically). Nevertheless, a model with chemically reasonable distances and angles was obtained. The most important distinguishing feature of the molecule is the mixed salicylato/acetato coordination mode. The two salicylates are bound to the Mn(III) ions along the tetragonally distorted axis.

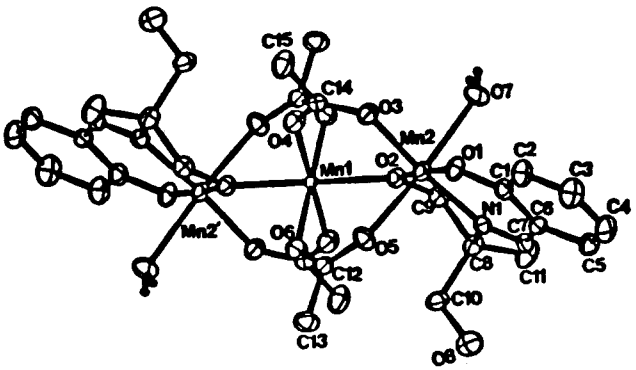

Figure 1. ORTEP diagram of **2** with 50% thermal ellipsoids showing the numbering scheme of the Mn(II) and Mn(III) first coordination sphere atoms. This molecule illustrates the basic structure of the linear isomers with the H_2O molecule occupying the variable solvent coordination site.

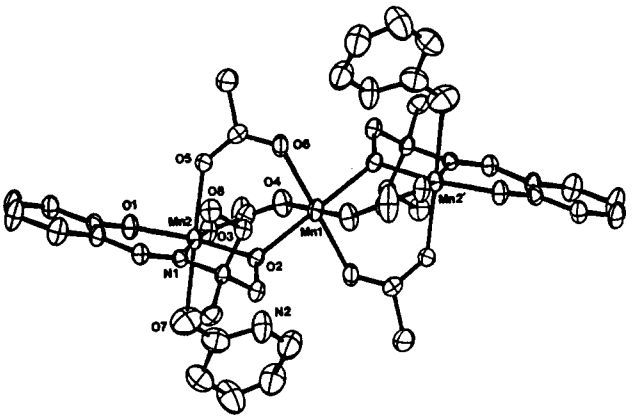

Figure 2. ORTEP diagram of **4** with 50% thermal ellipsoids showing the numbering scheme of Mn(II) and Mn(III) first coordination sphere atoms. This molecule contains a 2-hydroxypyridine which is oxygen bonded to the metal. The pyridine nitrogen atom (N2) is protonated, forming an internal hydrogen bond with the bridging alkoxide oxygen atom (O2).

The oxidation state assignments for Mn1 as an Mn(II) and Mn2 and Mn2′ as Mn(III) are based on the following observations. The trinuclear molecule is neutral and is composed of two dianionic ligands (e.g., SALADHP), four monoanionic carboxylate donors (e.g., acetates), and two neutral axial ligands. That the axial ligands are neutral, rather than the methoxide or hydroxide ions, was established by the successful isolation of $Mn^{II}Mn^{III}_2(SALADHP)_2(OAc)_4(THF)_2$, where the THF adduct must bind as a neutral donor. This complex has very similar solid state and identical solution behavior to **1** and **2**. Eight positive charges are required to render these compounds neutral, and this is accomplished by formal oxidation state assignments of two Mn(III) and one Mn(II). Given the symmetry of the molecules, Mn1 must be the Mn(II) and the terminal metal atoms are Mn(III). Additional support for this oxidation level is provided by the excellent fits to the variable-temperature magnetic data (vide infra) and X-ray absorption edge energies. Further, as discussed next, the solid state structures clearly show that these are valenced trapped materials based on bond lengths and the observed Jahn–Teller distortions.

Structural Description of Complexes. ORTEP diagrams of complexes **2** and **4** are shown as Figures 2 and 3, respectively. Chemically equivalent bond distances for the compounds are given in Table VI, and specific distances for the metal coordination sphere atoms of each structure are provided in Table VII. First, we will make a few general comments regarding the structure of these materials. The linear complexes (**1**–**4**) include a central, octahedral Mn(II) ion [Mn1] that is located on a crystallographic inversion center. It is flanked by two tetragonally distorted Mn(III) ions [Mn2]. The Mn(II) coordination sphere is composed of four syn bridging carboxylates and two μ-alkoxo oxygen atoms of the Schiff base ligand. Each Mn(III) is six coordinate using two syn bridging acetates, a tridentate Schiff base ligand, and a neutral axial donor. The Jahn–Teller distorted axes contain one carboxylate oxygen atom and the neutral monodentate ligand (O5 and O7 in Figure 1). The elongation is shown clearly by a comparison of Mn2–$O3_{av}$ (1.971 (9) Å) and Mn2–$O5_{av}$ (2.17 (1) Å) distances and by the long bond Mn2–$O7_{av}$ (2.32 (4) Å). In every complex, the SALADHP or SALATHM ligands are tridentate resulting in a meridional coordination geometry using an imine nitrogen and phenolate and alkoxide oxygen atoms to bind to the terminal Mn(III) ion. The meridional preference has been reported for other mono- and dinuclear manganese complexes with this and related ligands.[18,19,34] The Mn(III)–alkoxide oxygen distance (Mn2–$O2_{avg}$ = 1.880 (5) Å) is equivalent to the Mn(III)–phenolate oxygen distance (Mn2–$O1_{av}$ = 1.874 (4) Å), even though the former bridges to the Mn(II) ion. In addition, the Mn(III)–O2 distance is very similar to Mn(IV)–alkoxide oxygen bonds previously reported for $Mn^{IV}(SALADHP)_2$ (Mn–O_{av}, 1.889 Å)[18a] and $[Mn^{IV}(HIB)_3]^{2-}$ (Mn–O_{av}, 1.841 Å).[18d] As expected, there is a significant increase in the metal–alkoxide distance for Mn(II) (Mn1–$O2_{av}$, 2.140 Å). The Mn(II) octahedron is regular in both distances and angles. The Mn(III)–Mn(II) atoms are separated by very long distances with the shortest separation observed for the aqua complex, **2** (3.419 (1) Å), and the longest in **3** (3.515 (2) Å). The difference of 0.09 Å between complexes **1** (3.511 Å) and **2**, which differ solely by exchange of water for methanol, is probably due to a soft potential surface for these clusters. The effect is not primarily due to hydrogen bonding as complexes **1** and **2**, which exhibit the most significant deviations in metal separation, have similar hydrogen-bonding networks in the crystal. In the linear arrangement, the terminal manganese(III) atoms must be separated by twice these distances; however, in the bent isomer **5**,[6] the Mn(III)–Mn(II) separation is 3.502 (2) Å, and the Mn(III)–Mn(III) distance is 6.547 (4) Å as a result of the Mn(III)–Mn(II)–Mn(III) angle of 138.5 (2)°.

The stereochemical configuration of these trinuclear complexes can be viewed as $\{[Mn^{III}L(OAc)_2]_2\}Mn^{II}$ in which two complex monoanions, $[Mn^{III}L(OAc)_2]^-$, act as facial, tridentate chelating agents to the Mn(II). In this model, the linear isomers are formed as *trans*-$\{[Mn^{III}L(OAc)_2]_2\}Mn^{II}$, defined by the orientation of the bridging alkoxide, and the bent complex is *cis*-$\{[Mn^{III}L(OAc)_2]_2\}Mn^{II}$. The cis configuration induces a bent structure as a consequence of the average Mn1–O2–Mn2 angle of 121 (1)°. The two coordinated methanol molecules are oriented on the same side (syn) of the molecule in the bent (cis) isomer. In contrast, the neutral axial ligands of the linear (trans) isomers are arranged anti to one another. The Mn(III) ions are displaced slightly out of the best least squares plane defined by O1, N1, O2, and O3 toward the bridging acetate moiety by small, but significant amounts as reported in Table VII. As expected, the out of plane displacement decreases as the Mn(III)–O7 distance shortens. Specific comments concerning structures **1**, **2**, and **4** are provided below.

α-$[Mn^{II}Mn^{III}_2(SALADHP)_2(OAc)_4(CH_3OH)_2]\cdot 2CH_3OH$ (1). A brief description of this structure has appeared previously.[5] As shown in Table VII, this complex exhibits both the longest Mn(III)–Mn(II) separation of this series of compounds and the longest Mn(III)–O2 (alkoxide) bond. A slight disorder of the methyl and the uncoordinated hydroxymethyl groups of the SALADHP ligands was observed. The best model for this disorder gave occupancies of 0.70 and 0.30 for O8 (uncoordinated hydroxyl oxygen atom) and O8′, respectively.

(34) (a) Mikuriya, M.; Torihara, N.; Okawa, H.; Kida, S. *Bull. Chem. Soc. Jpn.* **1981**, *54*, 1063. (b) Tamura, H.; Ogawa, K.; Sakurai, T.; Nakahara, A. *Inorg. Chim. Acta* **1984**, *92*, 107. (c) Butler, K. D.; Murray, K. S.; West, K. O. *Aust. J. Chem.* **1971**, *24*, 2249. (d) Kessissoglou, D. P.; Butler, W. M.; Pecoraro, V. L. *Inorg. Chem.* **1987**, *26*, 495.

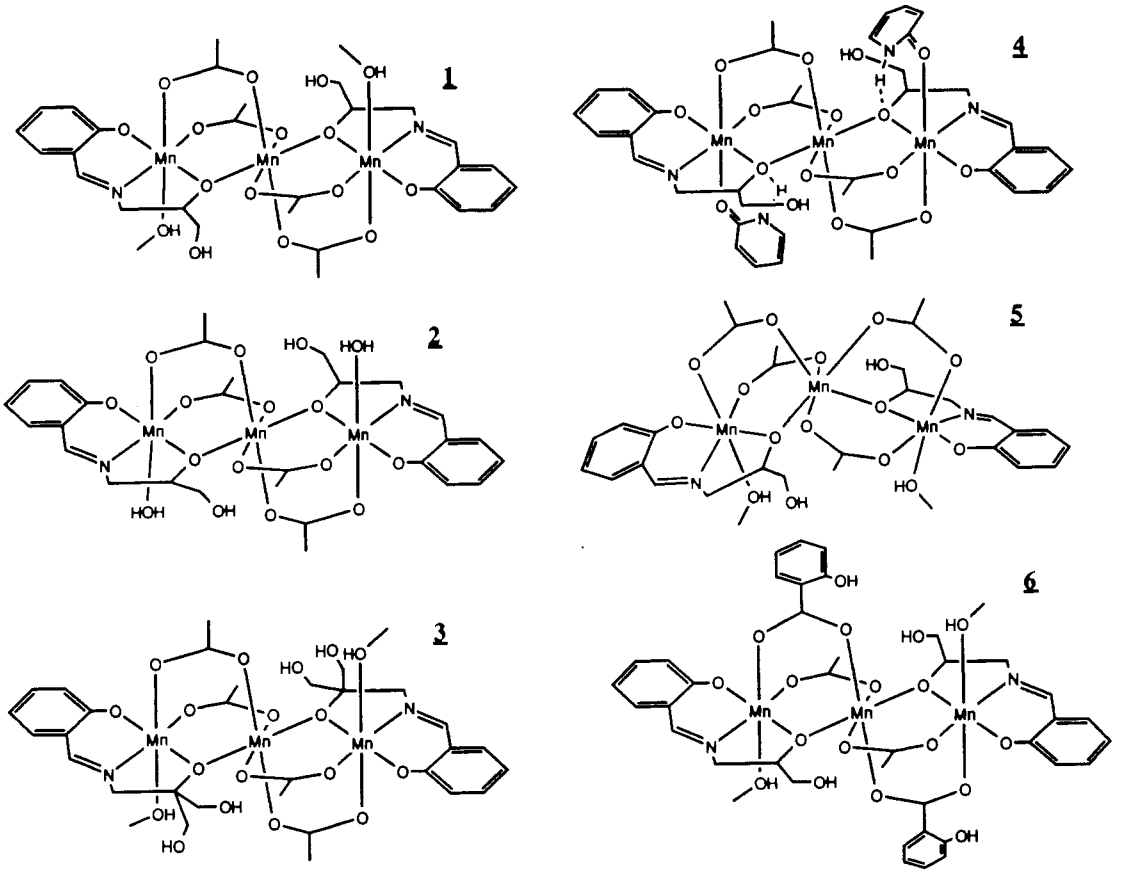

Figure 3. Structural representations of the six compounds used in this study.

Table VI. Important Average Distances and Angles for Structurally Characterized Trinuclear Complexes[a]

Mn2–O1	1.870–1.881 (1.875)	Mn2–O2	1.875–1.885 (1.880)
Mn2–O3	1.890–1.985 (1.957)	Mn2–O5	2.155–2.205 (2.177)
Mn2–O7	2.260–2.371 (2.304)	Mn2–N1	1.980–2.011 (1.992)
Mn1–O2	2.049–2.163 (2.140)	Mn1–O4	2.052–2.206 (2.169)
Mn1–O6	2.099–2.175 (2.156)	Mn1–Mn2	3.419–3.551 (3.504)
O1–Mn2–O2	172.3–176.2 (174.1)	O1–Mn2–O3	86.2–89.4 (88.2)
O1–Mn2–O2	87.9–91.9 (89.5)	O1–Mn2–O7	85.3–92.4 (88.8)
O1–Mn2–N1	90.7–91.9 (91.5)	O2–Mn2–N1	82.7–83.7 (83.2)
O2–Mn2–O3	95.4–99.2 (96.8)	O2–Mn2–O5	92.8–96.5 (94.4)
O2–Mn2–O7	83.6–90.5 (87.9)	O3–Mn2–O5	86.1–94.8 (90.5)
O3–Mn2–O7	80.0–88.5 (84.8)	O3–Mn2–N1	171.0–175.5 (173.4)
O5–Mn2–O7	174.0–176.1 (174.6)	O5–Mn2–N1	92.5–101.9 (95.4)
O7–Mn2–N1	86.4–92.0 (89.5)	Mn2–O2–Mn1	119.0–121.7 (120.8)
O2–Mn1–O4	86.0–89.2 (87.9)	O2–Mn1–O6	86.9–94.7 (91.8)
O4–Mn1–O6	90.3–92.7 (90.5)		

[a] Distances reported in Å, angles in deg. Values given are range for six structures. Values in parentheses are averages of chemically equivalent bonds in the six structures.

α-[$Mn^{II}Mn^{III}_2$(SALADHP)$_2$(OAc)$_4$(H_2O)$_2$]·H_2O·2CH_3OH (2). Compound **2** forms a structure very similar to that of **1**. In addition to the relatively short metal separation, **2** also shows the shortest Mn(II)–O2 distance of any of these compounds (Table VII). The angles of the heteroatoms forming the Mn–Mn bridges are altered only slightly going from **1** (Mn1–O2–Mn2 = 121.1 (2)°) to **2** (Mn1–O2–Mn2 = 120.9 (2)°). Structural characterization of H_2O–Mn(III) bonds are rare. The Mn–O distance in **2**, illustrated in Figure 2, is 2.271 (5) Å. This compares favorably with the Mn(III)–O distance of 2.29 Å for K[Mn(H_2O)$_2$(malonate)$_2$]·2H_2O[35] and is longer than the Mn(III)–water distances in [Mn_{12}(OAc)$_{16}$(H_2O)$_4O_{12}$]·4H_2O·2CH_3CO_2H[36] (2.18 Å) and $CsMnF_4$·2H_2O[37] (2.21 Å). Complexes **1** and **2** provide the first example of isostructural mixed valence manganese clusters which differ solely by the substitution of alcohol for water. The significance of this observation with respect to the photosynthetic water oxidizing system will be discussed below.

Table VII. Specific Distances and Angles for Structurally Characterized Trinuclear Complexes[a]

	Mn^{3+}–Mn^{2+}	Mn^{3+}–X	Mn^{3+}–O_a	Mn^{2+}–O_a	Mn^{3+}–O_a–Mn^{2+}	Mn(op)[b]
1	3.511	2.346	*1.885*	2.144	121.1	0.09 (1)
2	*3.419*	*2.271*	1.881	*2.049*	120.9	0.05 (1)
3	*3.515*	2.286	*1.876*	2.147	*121.7*	0.08 (1)
4	3.484	*2.371*	1.881	2.160	*119.0*	0.12 (1)
5[c]	3.502	2.333	1.884	*2.163*	119.6	0.10 (1)
av	3.486	2.321	1.881	2.133	120.5	0.09

[a] Distances reported in Å, angles in degrees. Italicized values represent maximum or minimum value. [b] Out of plane distance for Mn(III) toward the bridging acetate moiety. [c] The Mn^{3+}–Mn^{3+} distance is 6.547 Å; the Mn^{3+}–Mn^{2+}–Mn^{3+} angle is 138.5° as reported in ref 6.

Table VIII. Solid-State Magnetic Parameters for Trinuclear Complexes

compd	g_1	g_2[a]	J_{12}[b]	J_{22}[a]	zJ'[b]
1	2.05	2.0	–7.1	0.0	–0.5
2	2.08	2.0	–7.1	0.0	–0.65
3	2.03	2.0	–5.9	0.0	–0.4
4	2.01	2.0	–6.7	0.0	–0.5
5	2.10	2.0	–5.3	0.0	–0.7
6	2.08	2.0	–4.0	0.0	–0.9

[a] Fixed. [b] Reported in cm^{-1}.

α-[$Mn^{II}Mn^{III}_2$(SALADHP)$_2$(OAc)$_4$(HpyrO)$_2$]·H_2O·2HOpyr (4). Here, the methanol in **1** is displaced by 2-hydroxypyridine. Two

(35) Lis, T.; Matuszewski, J. *Pol. J. Chem.* **1980**, *54*, 163.
(36) Lis, T. *Acta Crystallogr.* **1980**, *B36*, 2042.
(37) Bhattacharjee, M. N.; Chaudhuri, M. K.; Dasgupta, H. S.; Khathing, D. T. *J. Chem. Soc., Dalton Trans.* **1981**, 2587; Edwards, A. J. *J. Chem. Soc., A* **1971**, 2653.

Scheme I

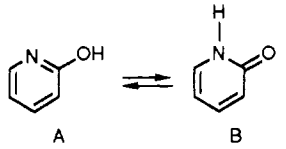

A B

tauteromeric forms for 2-hydroxypyridine are shown in Scheme I. The form with a protonated oxygen and an aromatic pyridine ring system is shown in structure A while the pyridine nitrogen is protonated and the exocyclic oxygen is ketonic in B. Thus, coordination to the Mn(III) can occur either through the ring nitrogen or the exocyclic oxygen. Examination of Figure 2 shows that 2-hydroxypyridine binds to the Mn(III) via the oxygen atom in tautomeric form B, reflecting the oxophilicity of manganese in this oxidation level. The 2-hydroxypyridine shows the longest Mn(III)–O7 distance (2.371 (1) Å) and the Mn(III) ions show the largest displacement (0.12 (1) Å) from the best least squares plane of O1–N1–O2–O3. The pyridine nitrogen is protonated and forms an internal hydrogen bond with the deprotonated, bridging alkoxide oxygen atom, O2.

Magnetic Studies of the Trinuclear Materials. The Heisenberg exchange Hamiltonian for a trinuclear arrangement of coupled spins is given by

$$\mathcal{H}_{ex} = -2J_{22'}S_2\cdot S_{2'} - 2JS_{22'}\cdot S_1$$

where the spins ($S_1 = 5/2$ and $S_2 = S_{2'} = 2$) are arranged in the order S_2–S_1–$S_{2'}$ to reflect the symmetry of S_2 being equivalent to $S_{2'}$. In the case of the trinuclear complexes studied here, the arrangement is linear and $J_{22'}$ is expected to be negligible. Therefore, the major exchange interaction is expected between the terminal (Mn2 and Mn2′) and central (Mn1) metals. This interaction is designated as J (where $J = J_{12} = J_{12'}$). Vector coupling of the spins results in the exchange Hamiltonian being diagonal in S^2 and $S_{22'}^2$. The exchange energies may be calculated by Kambe's method,[38] and the energies in the limit of $J_{22'}$ being zero are given by

$$E(S,S_{22'}) = J[S_{22'}(S_{22'} + 1) + S_1(S_1 + 1) - S(S + 1)]$$

where the allowed values of the resultants are given by the triangle relation.

The Zeeman Hamiltonian is

$$\mathcal{H}_{Zeeman} = \mu_B(g_2S_{22'} + g_1S_1)\cdot\mathbf{B}$$
$$= \mu_B[g_2S + (g_1 - g_2)S_1]\cdot\mathbf{B}$$

and is diagonal in S^2 and $S_{22'}^2$ only if $g_2 = g_1$. Since the g values for Mn(II) and Mn(III) are expected to differ, there will be off-diagonal matrix elements of the form

$$\langle S_{22'}SM|S_{22'}|S_{22'}'S'M'\rangle$$

The first- and second-order contributions to the Van Vleck equation are[39,40]

$$\Sigma_M E_1^2 = {}^1/_3S(S + 1)(2S + 1)[g_2 - (g_1 - g_2)]\sigma(S)$$

and

$$\Sigma_M E_2 = {}^1/_3(g_1 - g_2)^2\mu_B{}^2\Sigma_{s'}\tau(S,S')/E(S,S')$$

where

$$\sigma(S) = [S_{22'}(S_{22'} + 1) - S_1(S_1 + 1) - S(S + 1)]/2S(S + 1)$$

$$\tau(S,S') = (S_{22'} + S_1 + 1 + \bar{S})(S_{22'} + S_1 + 1 - \bar{S})(\bar{S} + S_{22'} - S_3)(\bar{S} + S_{22'} - S_3)/4\bar{S}$$

$$E(S,S') = E_0(S,S_{22}) - E_0(S',S_{22})$$

Here, $\bar{S}$ is the larger of S and S'. Finally, a mean field correction of the form

$$\chi/(1 - 2zJ'\chi/N\mu_B{}^2g^2)$$

was added to account for intercluster interactions.

The magnetic parameters obtained from the best-fit calculations are collected in Table VIII. Because of the large number of parameters and the availability of data for powdered samples only, two of the parameters were fixed at constant values. First, the g value of manganese(II), g_3 in our notation, was fixed at the value of 2.0. This is a reasonable g value for high-spin manganese(II) in a ^{6}A state. Inspection of tables of g values for manganese(II) in any of a number of compilations reveals that the g value typically differs from 2.0 only in the thousandth place.[41]

The second parameter that was held constant, at 0.0 cm^{-1}, was the exchange coupling between the terminal manganese(III) ions, this being $J_{22'}$ in our notation. This was a reasonable assumption considering the distance between the two terminal paramagnetic ions and the absence of likely superexchange pathways between the ions. Calculations in which this parameter was allowed to vary invariably returned the same best-fit values for the other parameters and a range of very small values for $J_{22'}$.

A plot of the experimental data for **1** (α-$Mn_3(SALADHP)_2(OAc)_4(CH_3OH)_2\cdot 2CH_3OH$) is given in Figure 4. The lines drawn through the data points were generated by the best-fit parameters in Table VIII and the theoretical expressions described above. Equally good fits to the data were obtained for the other five compounds by using the best-fit parameters. Plots of these data and the best-fit lines are deposited in the supplementary material as Figures 10–14.

The magnetic data reveal, through the near constancy of J for compounds **1–3** and **5**, that exchange coupling between the terminal manganese(III) ion and the central manganese(II) ion is insensitive to the identity of the terminal ligand or to the overall geometry of the trimeric molecule. α-$Mn_3(SALADHP)_2(OAc)_4(CH_3OH)_2\cdot 2CH_3OH$ is linear and has $J = -7.1$ cm^{-1}, and β-$Mn_3(SALADHP)_2(OAc)_4(CH3OH)_2\cdot 4HOpyr$ is bent and has $J = -6.7$ cm^{-1}. The decrease in J to -5.9 cm^{-1} in $Mn_3(SALATHM)_2(OAc)_4(CH_3OH)_2\cdot H_2O\cdot 2CH_3OH$ might reflect the presence of the third hydroxyl group, but we are not inclined to present such an argument. However, the decrease of J to -5.3 cm^{-1} for **4** is real and reflects the presence of the hydroxypyridine ligand. The crystallographic data, discussed above, reveal meaningful differences in the metric parameters, and there is intramolecular hydrogen bonding with the bridging alkoxide ligand. The hydrogen bonding perturbs the electron density on the bridge adequately to diminish superexchange by this route.

The reduction in the exchange coupling constant $|J|$ for compound **6** ($Mn_3(SALADHP)_2(OAc)_2(salicylato)_2(CH_3OH)_2\cdot 4H_2O$) is real and may be understood in terms of the substituents on the bridging carboxylate groups. Compounds **1–5** have two acetate groups bridging the manganese ions, while compound **6** has one acetate bridge and one salicylate bridge. The electron-withdrawing nature of the hydroxyphenyl group removes electron density from the carboxylate function, and superexchange interactions by way of these bridges are diminished relative to those with the carboxylate groups which have electron-donating methyl groups as substituents.

Finally, the magnetic studies on this group of six compounds permitted the proper assignment of oxidation states to the terminal

(38) Kambe, K. *J. Phys. Soc. Jpn.* **1950**, *5*, 48.
(39) (a) Yablokov, Y. V.; Gaponenko, V. A.; Eremin, M. V.; Zelentsov, V. V.; Zemchuzhnikova, T. A. *Sov. Phys.-JETP* **1974**, *38*, 988.
(40) Blake, A. B.; Yavari, A.; Hatfield, W. E.; Sethulekshmi, C. N. *J. Chem. Soc., Dalton Trans.* **1985**, 2509.
(41) Al'tshuler, S. A.; Kozyrev, B. M. *Electron Paramagnetic Resonance of Transition Elements*; 2nd ed.; John Wiley & Sons: New York; 1972; p 317 ff.

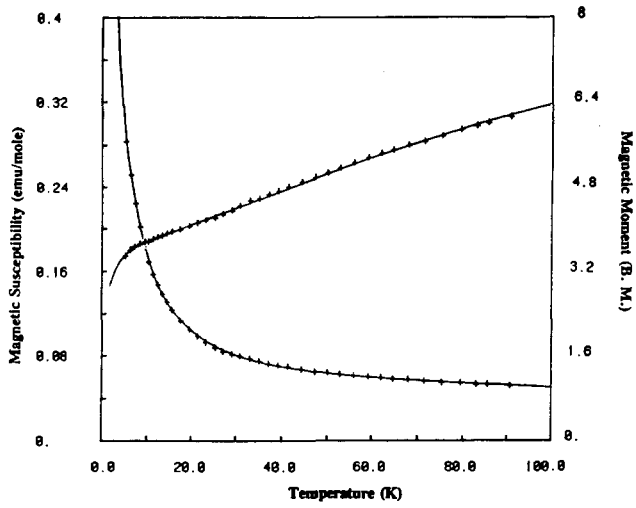

Figure 4. Variable temperature magnetic susceptibility data for α-[$Mn^{II}Mn^{III}_2$(SALADHP)$_2$(OAc)$_4$(CH_3OH)$_2$]·2CH_3OH (**1**).

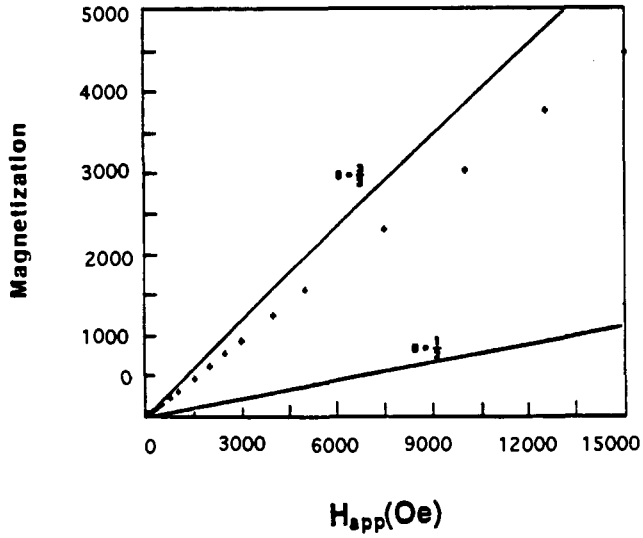

Figure 5. Magnetization study for α-[$Mn^{II}Mn^{III}_2$(SALADHP)$_2$(OAc)$_4$(CH_3OH)$_2$]·2CH_3OH (**1**) at 4.2 K over the field range 0–15 000 G.

manganese ions. An alternate assignment in **1**, for example, would have coordinated methoxide, thus leading to a conclusion that the terminal manganese ions were in oxidation state IV. Numerous attempts to simulate the magnetic data in these terms failed.

A calculation of the energies of all the states arising from exchange coupling in the trimeric system as a function of the antiferromagnetic exchange coupling constant J indicated that an $S = {}^1/_2$ state is the ground state up to a value of $|J| = 0.4$ cm^{-1}, at which energy there is a ground-state cross-over with an $S = {}^3/_2$ state becoming the ground state. The $|J|$ value determined from our analysis of the magnetic susceptibility data is well into the $S = {}^3/_2$ ground-state regime, with the $S = {}^1/_2$ state lying at a slightly higher energy. This arrangement of states was verified experimentally from isothermal magnetization measurements at 4.2 K. The data are given in Figure 5, where the experimental points are indicated with +'s. The theoretical magnetization behavior for an $S = {}^1/_2$ state and for an $S = {}^3/_2$ state, calculated from the expression

$$M = Ng\mu_B S \cdot B_s(x)$$

where $B_s(x)$ is the Brillouin function for states with $S = {}^3/_2$ and $S = {}^1/_2$, are shown as solid lines in Figure 5. The data and theoretical results clearly reflect that the lowest lying state has $S = {}^3/_2$ with a reasonable population of a state, or states, of lower spin causing the deviation of the observed magnetization from that predicted for a singlely populated $S = {}^3/_2$ state. In view of the large number of other low-lying states, no attempt was made to simulate the experimentally observed magnetization behavior.

Discussion

Relationship of Manganese Oxidation State to the Metal/Alkoxide Ratio. A distinct trend in metal oxidation state for manganese alkoxide complexes can now be discerned from the structures of manganese SALADHP and related complexes. Air-stable mononuclear manganese(IV) complexes can be achieved in materials such as $Mn(HIB)_3^{2-}$ or $Mn(SALADHP)_2$ that contain ratios of two or greater alkoxides per manganese. Three distinct Mn(III) dimers can be formed with similar, but nonidentical environments. In [Mn(2-OH-SALPN)]$_2$$CH_3OH$[19] (**8**), the coordination sphere of Mn1 is nearly identical to that in $Mn(SALADHP)_2$ except that one of the alkoxide oxygen atoms is bridging to another metal. This leads to a destabilization of the Mn(IV) oxidation level by nearly 700 mV. Mikuriya et al.[34a] have synthesized [Mn(SALAHP)(OAc)]$_2$ (**9**), and we have structurally characterized [Mn(SALAHP)(CH_3OH)Cl]$_2$ (**10**).[19d] In both cases, the dimer is formed by two bridging alkoxides between the manganese giving an alkoxide to manganese ratio of 1:1. It should also be noted that stable Mn(II) dimers can be prepared with 1:1 phenoxide ratios.[34c,d] The trinuclear compounds reported herein are even more alkoxide deficient, with a ratio of 0.67:1 and an average oxidation state of 2.67. This trend is not simply a result of the phenolate or imine ligands since Mn(SALGLY)$_2$, which uses carboxylate residues in place of the alkoxides but retains the two phenolates and imines, is stable as the Mn(III) complex.[34b] Thus, we conclude that high-valent manganese clusters can be achieved when employing alkoxide moieties; however, in general more than one alkoxide is required per manganese to achieve the Mn(IV) oxidation level.

Relationship to the Photosynthetic Water-Oxidizing Enzyme. The wide range of structural proposals for active site nuclearity in the OEC are based on EPR[42] and X-ray absorption[43] spectroscopies and synthetic modeling studies. Single center proposals (tetranuclear) incorporating asymmetric cubanes,[44] butterfly clusters,[45] or dimers of dimers[43c] are among the more likely metal aggregations in this enzyme. Very recently, the stoichiometry of Mn/OEC has been reevaluated and a value of 6 has been forwarded.[46] *If this quantification stands the test of further scrutiny*, an attractive model would be a dimer of trimers. Three possible metal–metal separations are seen in the EXAFS data. The shortest is at 2.7 Å[43] (1–1.5 scatterers/Mn), an intermediate distance at 3.3 Å is also apparent[43] (0.5 scatterer/Mn), and the possibility of a much longer metal–metal separation at 4.5 Å (0.5 scatterer/Mn) has been suggested.[43e] It is clear from these distances that the trinuclear compounds **1–6** are not appropriate structural models for the manganese in the oxygen-evolving complex. However, the compounds still may provide

(42) (a) Dismukes, G. C.; Siderer, Y. *Proc. Natl. Acad. Sci. U.S.A.* **1981**, *78*, 274. (b) Casey, J.; Sauer, K. *Biochem. Biophys. Acta* **1984**, *767*, 21. (c) dePaula, J. C.; Beck, W. F.; Brudvig, G. W. *J. Am. Chem. Soc.* **1986**, *108*, 4002. (d) Hansson, O. R.; Aasa, R.; Vanngard, T. *Biophys. J.* **1987**, *51*, 825. (e) Zimmermann, J.-L.; Rutherford, A. W. *Biochemistry* **1986**, *25*, 4609.

(43) (a) Cole, J. L.; Yachandra, V. K.; McDermott, A. E.; Guiles, R. D.; Britt, R. D.; Dexheimer, S. L.; Sauer, K.; Klein, M. P. *Biochemistry* **1987**, *26*, 5967. (b) Yachandra, V. K.; Guiles, R. D.; McDermott, A.; Britt, R. D.; Dexheimer, S. L.; Sauer, K.; Klein, M. P. *Biochim. Biophys. Acta* **1986**, *850*, 324. (c) George, G. N.; Prince, R. C.; Cramer, S. P. *Science* **1989**, *243*, 789. (d) Yachandra, V. K.; Guiles, R. D.; McDermott, A.; Cole, J. L.; Britt, R. D.; Dexheimer, S. L.; Sauer, K.; Klein, M. P. *Biochemistry* **1987**, *26*, 5974. (e) Penner-Hahn, J. E.; Fronko, R.; Pecoraro, V. L.; Bowlby, N.; Yocum, C. F. *J. Am. Chem. Soc.* **1990**, *112*, 2549.

(44) Brudvig, G. W.; Crabtree, R. H. *Proc. Natl. Acad. Sci. U.S.A.* **1986**, *83*, 4586.

(45) Vincent, J. B.; Christou, G. *Inorg. Chim. Acta* **1987**, *136*, L41.

(46) Pauly, S.; Witt, H. T. *Biochim. Biophys. Acta* **1992**, *1099*, 211.

useful information for magnetostructural correlations of mixed-valence manganese clusters using heteroatom donors in geometries that may be somewhat similar to the biological system. In particular, they are useful in defining the sensitivity of magnetic exchange to ligand type and orientation.

The addition of ethanol to OEC preparations is responsible for a shift in the relative signal intensities of the $g = 4.1$ and the $g = 2$ multiline signals in the S_2 oxidation level of this enzyme.[42] The conversion from the low-field signal ($g = 4.1$) to the doublet component ($g = 2$ multiline) has been attributed to a cluster conformational change.[42c] At present, it is unknown whether added alcohols directly interact with the manganese cluster or simply induce a protein conformational change that perturbs the active site. However, anions that are also known to perturb the relative intensities of the two EPR signals are thought to bind directly to the manganese ions.

This trinuclear system is the first to examine the effects on the magnetic interactions in a manganese cluster in which the only modification is the simple exchange of water for an alcohol. Neither perturbation of the magnetic exchange nor an alteration in the ground magnetic state are observed between **1** and **2**. In fact, the magnetic properties of this entire class of mixed valence complexes appear to be insensitive to nearly all structural changes including alteration of metal–metal distances, metal–metal angles, alkoxide bridging angles, out-of-plane displacement of Mn(III), and the neutral axial coordinated ligands. The only significant perturbation is associated with electron-donating or -withdrawing substituents on the carboxylate ligands. This is probably a reflection of the electronic symmetry of Mn(III) which has a magnetic orbital oriented directly at the bridging acetates. The substitution of salicylate for acetate modifies the superexchange pathway and the coupling decreases. Apparently, the weak neutral, axial ligands do not vary sufficiently in donor capacity to perturb the energy of the d_{z^2} orbital significantly. Therefore, no effect is seen on axial donor substitution. Furthermore, marked changes in exchange coupling and ground state configuration might not be expected in this system because magnetic exchange is usually very weak in low-valent Mn clusters.

Acknowledgment. The authors wish to express their appreciation to Dr. William Butler for his invaluable technical and moral assistance provided in support of this work. This research was supported by NIH Grant GM-39406 (D.P.K., M.S.L., X.L., and V.L.P.) and NSF grant CHE88 07498 (M.L.K. and W.H.). V.L.P. thanks the G. D. Searle Family/Chicago Community Trust for a Biomedical Research Scholar's Award (1986–1989) and The Alfred P. Sloan Foundation for a Sloan Fellowship (1989–1991).

Supplementary Material Available: Table S9, providing a complete crystallographic summary for **1**–**4**, listings of fractional atomic positions for hydrogen atoms, anisotropic thermal parameters for all non-hydrogen atoms, isotropic thermal parameters for hydrogen atoms, a complete set of bond distances, and a complete set of bond angles for **1** (Tables 10–14), **2**, (Tables 16–20), **3** (Tables 22–26), **4** (Tables 28–32), **5** (Tables 34–38), and **6** (Tables 40–44), Figures 6–9, providing complete numbering schemes for all atoms, and Figures 10–14, giving magnetic data for compounds **2**–**6** (61 pages). Ordering information is given on any current masthead page.